BROOKHAVEN
NATIONAL LABORATORY

BNL-77075-2006-CP

High spatial-resolution imaging of Te Inclusions in CZT material

G. S. Camarda[a*], A. E. Bolotnikov[a], G. A. Carini[a], Y. Cui[a], K. T. Kohman[b], L. Li[c], and R. B. James[a]

[a]Brookhaven National Laboratory, Upton, NY 11973
[b]Kansas State University, Manhattan, KS 66506
[c]Yinnel Tech, Inc., 3702 West Sample Street, South Bend, IN 46619

SPIE, Hard X-ray and Gamma-Ray Detectors Physics VIII
San Diego, California
August 13th-17th, 2006

Nonproliferation and National Security Department
Detector Development and Testing Division

Brookhaven National Laboratory
P.O. Box 5000
Upton, NY 11973-5000
www.bnl.gov

*giuseppec@bnl.gov; phone 631-344-2008; fax 631-344-3374

DISCLAIMER

High spatial-resolution imaging of Te Inclusions in CZT material

G. S. Camarda[a*], A. E. Bolotnikov[a], G. A. Carini[a], Y. Cui[a], K. T. Kohman[b], L. Li[c], and R. B. James[a]

[a]Brookhaven National Laboratory, Upton, NY 11973

[b]Kansas State University, Manhattan, KS 66506

[c]Yinnel Tech, Inc., 3702 West Sample Street, South Bend, IN 46619

ABSTRACT

We present new results from our studies of defects in current single-crystal CdZnTe material. Our previous measurements, carried out on thin (~1 mm) and long (>12 mm) CZT detectors, indicated that small (1-20 μm) Te inclusions can significantly degrade the device's energy resolution and detection efficiency. We are conducting detailed studies of the effects of Te inclusions by employing different characterization techniques with better spatial resolution, such as quantitative fluorescence mapping, X-ray micro-diffraction, and TEM. Also, IR microscopy and gamma-mapping with pulse-shape analysis with higher spatial resolution generated more accurate results in the areas surrounding the micro-defects (Te inclusions). Our results reveal how the performance of CdZnTe detectors is influenced by Te inclusions, such as their spatial distribution, concentration, and size. We also discuss a model of charge transport through areas populated with Te inclusions.

Keywords: CdZnTe, Te inclusions, gamma-ray detectors

1. INTRODUCTION

It has long been known that grain boundaries and twins degrade the performance of a device, and hence, a first step in material screening is to ensure that CZT crystals are free of these macroscopic defects. However, the role of the Te inclusions remained obscure. By using synchrotron radiation at the National Synchrotron Light Source (NSLS), we recently demonstrated that single Te inclusions trap a significant amount of charge of an electron cloud. Te inclusions and their surrounding areas were measured, and the deleterious effects of Te inclusions on the energy spectrum were unambiguously observed [1-4]. However, it still is not known to what extent these inclusions affect the spectral response of CZT detectors. Here, we quantitatively affirm that a poor spectral response, observed with some fabricated Frisch ring detectors, correlates with high concentrations of inclusions that cause large fluctuations of the collected charge.

Simulations [5] of charge transport through areas containing Te inclusions indicated that their cumulative effects can explain the degradation of energy resolution in thick CZT devices. The goal of this work was to experimentally correlate the size and concentrations of Te inclusions with the devices' responses. The sizes and concentrations of the Te inclusions were measured with an automated IR imaging system developed at BNL to screen CZT crystals. This system is described, and the findings from CZT crystals from several growers are presented. These results are used to predict the

*giuseppec@bnl.gov; phone 631-344-2008; fax 631-344-3374

extent to which Te inclusions can be tolerated. The experimental results agree well with those obtained from modeling.

2. EXPERIMENTAL SETUP

Figure 1 (a) illustrates the automated IR imaging system that we developed to accurately record the size and number of the Te inclusions in the volume of CZT crystals. CZT crystals are opaque to visible light but transparent if illuminated with IR light. A fiber-optic illuminator together with a collimator initially was utilized to illuminate the CZT sample under test. To improve the uniformity of the illumination, subsequently we used a LED backlight, but regardless of the type of source used it proved extremely difficult, nigh impossible, to obtain a perfectly even pattern of illumination on the object. Illumination and optical non-uniformities negatively impact the quality of images captured. We minimized these effects, and often eliminated them by undertaking a proper flat-field calibration of the system's CCD camera.

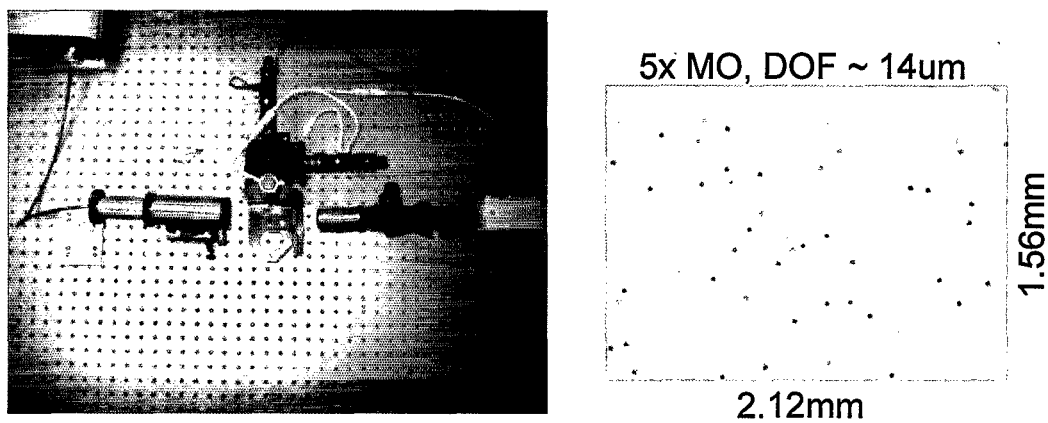

Fig. 1. Top view of the automated IR imaging system (a). An IR micrograph image taken with a 5x magnification microscope objective (b). The field of view is 2.12x1.56 mm, and the depth of focus is 14 um.

CZT crystals of different dimensions and grown by different techniques were acquired from several vendors. Their surfaces were polished if this had not been done before purchase. The CZT crystal to be inspected was placed on a XYZ motorized translation stage with a resolution of 0.1 um. The three actuators are controlled via a PC using serial connectors. The software to communicate with the actuators was developed and written at BNL using a VC++ programming environment. A large field-of view microscope objective, a CCD camera, and an in-line optic assembly system then were mounted in line with the XYZ translation stages and the backlight fiber optic. The in-line system is needed to mount the infinite-conjugate microscope objectives to the CCD camera.

Long working-distance objectives with magnifications (field-of-view (FOV)) from 2x (h 5.3mmx v 3.8mm) to 20x (h 0.53mm x v 0.38mm) were used.

The CCD camera has a sensor of 7.8 mm x 10.6 mm area and provides 2208x3000 pixels, each of 3.5 um. The camera is connected to the PC by firewire cable and was controlled, as were the actuators, with C++ software specifically written for this task. The firewire connection allowed us to take, and save high-resolution images very quickly, and so the total time required to scan a large volume of the CZT was very short.

The system can perform a one-, two-, or three-dimensional raster scan of a CZT crystal. At each XYZ-position an image is taken and saved, and then the translation stages move the sample to the next position where the picture of the new area is taken, and so on. The step size of the raster scan depends on the FOV adopted.

The system was principally utilized to measure the size and the concentration of Te inclusions per cm^3 of CZT crystals grown by different techniques. We describe below the iterative algorithm that was developed to locate Te inclusions in the images and identify their shapes and sizes. To determine the concentration of Te inclusions per cm^3, after choosing a particular xy area, we performed a one-dimensional scan in the z direction (in depth). For example, considering a 5 mm-thick CZT sample, and using a 50 um z-scan step, 100 different images were acquired. Ideally, these 100 IR micrographs can be stitched together in the z direction to form a known volume of CZT, and then the concentration of Te inclusions can be obtained by counting how many such inclusions there are in the volume analyzed. For each CZT sample, five different measurements were taken at five different locations over the crystal's length from two perpendicular directions.

When scanning in the z direction, the step size for the scan depends on the microscope objective's depth of focus (DOF). For example, by using a 5x magnification, the associated DOF was 14 um.

After the scan in the z direction, 100 images were ready for analysis. The iterative algorithm developed to locate Te inclusions in the images and identify their shapes and sizes is described next.

3. METHOD (ALGORITHM) AND RESULTS

CZT crystals are opaque to visible light but are transparent to IR light, whilst, in contrast, Te inclusions are opaque to both visible and IR, so they appear black in a IR micrograph (see Figure 1 (b)). Our goal was to measure the concentrations of Te inclusions per cm^3. The algorithm used to count the Te inclusions and to measure their size was developed with Interactive Data Language (IDL). After obtaining the z scans (i.e., scans in the z direction), as a first step we converted each image to its negative, so in fact, we analyze the negative of the original image. Each image has large objects with relatively low brightness (out-of-focus Te inclusions), and compact objects with high brightness (in-focus Te inclusions) as in Figure 1 (b) and Figure 2, where the radius of the Te inclusions versus their brightness is shown. In Figure 2, three regions can be marked out. Region 1 regroups objects (Te inclusions) of small radius and high brightness; region 3 regroups objects with large radius and low brightness, and finally, region 2, between region 1 and 3 collects objects with medium size and medium brightness.

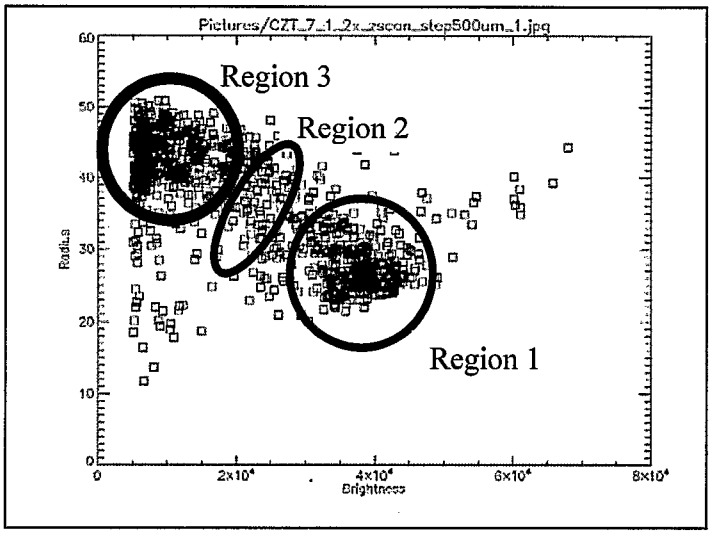

Fig. 2 Distribution of the radius of the Te inclusions (the objects) versus brightness. Region 1 regroups objects (Te inclusions) of small radius and high brightness; region 3 regroups objects with large radius and low brightness, and finally, region 2, between region 1 and 3 collects objects with medium size and medium brightness.

The goal of the algorithm is to discard Te inclusions that are out of focus and count only those in focus. This requires two steps. First, a cutoff is applied on brightness to suppress the contribution of objects of low brightness (Te inclusions out of focus) on the negative, i.e., Te inclusions in region 3 are discarded. The second step is where the algorithm selects only one of the Te inclusions present at the same position in 3-5 different layers (the number depending on the DOF). For clarity we use layer instead of image here. The same Te inclusion can appear in several neighboring layers (i.e. in both region 1 and 2), but would be in focus only in one layer, or at least there would be a layer where that inclusion is in better focus than in the others. The algorithm selects the one in focus, and corrects also for shifts of images. In this way, the algorithm ensures we count each Te inclusion only once.

Now, knowing the FOV, the size of the z-scan step and the number of Te inclusions for each layer, the concentration of Te inclusions can be calculated. For each CZT sample, five different measurements were taken at five different locations over the crystal's length from two perpendicular directions. Then their average gives the concentration per cm^3.

The algorithm also records the size of each Te inclusion counted. Figure 3 is a histogram of the sizes of the Te inclusions sizes (FWHM of the intensity peak corresponding to the inclusion) for a CZT crystal.

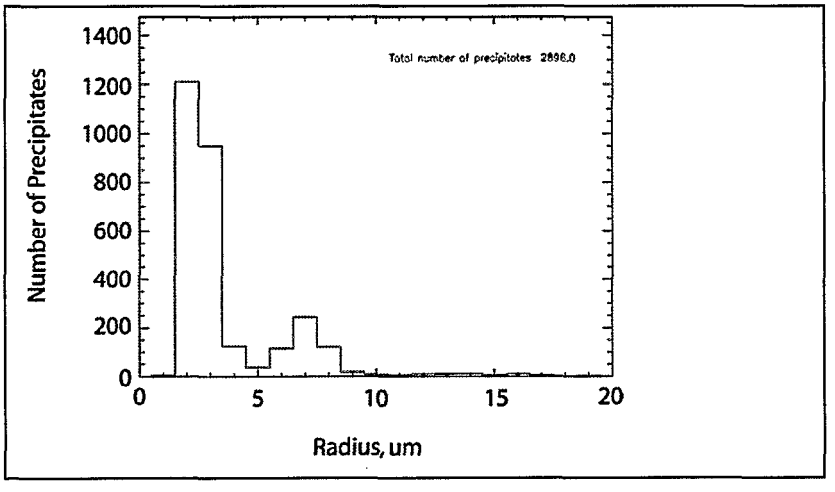

Fig.3 Histogram of the Te inclusion sizes.

So far, five CZT crystals have been measured, and Table 1 summarizes our preliminary results. The concentration per cm^3, size, and FWHM with a ^{137}Cs source for 662 keV are shown.

Detector	Concentration (Inclusions/cm^3)	Size (μm)	FWHM @ 662keV
1	9.8E+04	From 3 to ~20	6.2%
2	9.6E+04	From 3 to ~10	3.8%
3	4.9E+04	From 2 to <10	1.2%
4	2.7E+06	< 3	1.4%
5	1.2E+06	< 3	0.8%

Table 1 Concentration, size, and energy resolution of five CZT crystals.

The energy resolution was obtained by assembling the crystal in a Frisch ring detector configuration. CZT crystals with a high concentration of Te inclusions of about 15 um in size perform worse than crystals with lower concentrations of similar sized Te inclusions.

CZT crystals with small Te inclusions, of about 2 um, and a high concentration of Te inclusions, of about 10^6, can give the same or better energy resolution than crystals with larger Te inclusions and lower concentrations per cm^3. These are preliminary results and more measurements are needed to confirm the findings. These results agree well with the simulation results [5].

4. CONCLUSIONS

In this work we demonstrated that CZT crystals with small Te inclusions and a high concentration can give the same or better energy resolution than crystals with larger Te inclusions and lower concentrations per cm^3. Also we observed that CZT crystals with Te inclusions smaller than 2 um and concentrations lower than 10^6 do not affect significantly the detector's performance. A FWHM of less than 1% was obtained for 662 keV. Strong correlations between the inclusions' size, concentrations, and the device's spectral response were found. Our preliminary experimental results agree well with those obtained from modeling. This correlation can be used to predict CZT devices performance and moreover to understand material issues that represent factors limiting their performance.

ACKNOWLEDGEMENTS

This work was supported by U.S. Department of Energy, Office of Nonproliferation Research and Engineering, NA-22. The manuscript has been authored by Brookhaven Science Associates, LLC under Contract No. DE-AC02-98CH1-886 with the U.S. Department of Energy. The United States Government retains, and the publisher, by accepting the article for publication, acknowledges, a world-wide license to publish or reproduce the published form of this manuscript, or allow others to do so, for the United States Government purposes.

REFERENCES

[1] G. S. Camarda, A. E. Bolotnikov, G. A. Carini, L. Li, G. W. Wright, and R. B. James, "The Effects of Precipitates on CdZnTe Device Performance", in Proceedings of SPIE Hard X-Ray and Gamma-Ray Detector Physics VII, edited by R. B. James, L. A. Franks, and A. Burger (SPIE, Bellingham, WA, 2005), 592004-1 – 592004-7.

[2] G. A. Carini, A. E. Bolotnikov, G. S. Camarda, G. W. Wright, L. Li, and R. B. James, "Effect of Te inclusions on the performance of CdZnTe detectors", Appl. Phys. Lett. 88, p. 143515, 2006.

[3] G. S. Camarda, A. E. Bolotnikov, G. A. Carini, and R. B. James, "Effects of Tellurium Inclusions on charge collection in CZT Nuclear Radiation Detectors", in Countering Nuclear and Radiological Terrorism, edited by S. Aprkyan and D. Diamond, Springer, 2006, pp. 199-207.

[4] G. A. Carini, A. E. Bolotnikov, G. S. Camarda, R. B. James, "High-resolution x-ray mapping of CdZnTe detectors", submitted to Nucl. Instr. Meth., 2006.

[5] A. E. Bolotnikov, G. S. Camarda, , G. A. Carini, Y. Cui, K. T. Kohman, L. Li, M. B. Salomon, and R. B. James, "The effect of Te inclusions on characteristics of CdZnTe detectors", SPIE 6319A, San Diego 2006, in this proceedings.